Physics in Medicine & Biology

IPEM Institute of Physics and Engineering in Medicine

ACCEPTED MANUSCRIPT • OPEN ACCESS

Delivery time reduction for mixed photon-electron radiotherapy by using photon MLC collimated electron arcs

To cite this article before publication: Gian Guyer *et al* 2023 *Phys. Med. Biol.* in press https://doi.org/10.1088/1361-6560/ad021a

Delivery time reduction for mixed photon-electron radiotherapy by using photon MLC collimated electron arcs

Gian Guyer[1], Silvan Mueller[1], Paul-Henry Mackeprang[1], Daniel Frei[1], Werner Volken[1], Daniel M. Aebersold[1], Kristina Loessl[1], Peter Manser[1], Michael K. Fix[1]

[1] Division of Medical Radiation Physics and Department of Radiation Oncology, Inselspital, Bern University Hospital, and University of Bern, Bern, Switzerland

E-mail: gian.guyer@insel.ch

Abstract.

Objective: Electron arcs in mixed-beam radiotherapy (Arc-MBRT) consisting of intensity-modulated electron arcs with dynamic gantry rotation potentially reduce the delivery time compared to mixed-beam radiotherapy containing electron beams with static gantry angle (Static-MBRT). This study aims to develop and investigate a treatment planning process (TPP) for photon multileaf collimator (pMLC) based Arc-MBRT.

Approach: An existing TPP for Static-MBRT plans is extended to integrate electron arcs with a dynamic gantry rotation and intensity modulation using a sliding window technique. The TPP consists of a manual setup of electron arcs, and either static photon beams or photon arcs, shortening of the source-to-surface distance for the electron arcs, initial intensity modulation optimization, selection of a user-defined number of electron beam energies based on dose contribution to the target volume and finally, simultaneous photon and electron intensity modulation optimization followed by full Monte Carlo dose calculation. Arc-MBRT plans, Static-MBRT plans, and photon-only plans were created and compared for four breast cases. Dosimetric validation of two Arc-MBRT plans was performed using film measurements.

Main results: The generated Arc-MBRT plans are dosimetrically similar to the Static-MBRT plans while outperforming the photon-only plans. The mean heart dose is reduced by 32% on average in the MBRT plans compared to the photon-only plans. The estimated delivery times of the Arc-MBRT plans are similar to the photon-only plans but less than half the time of the Static-MBRT plans. Measured and calculated dose distributions agree with a gamma passing rate of over 98% (3% global, 2 mm) for both delivered Arc-MBRT plans.

Significance: A TPP for Arc-MBRT is successfully developed and Arc-MBRT plans showed the potential to improve the dosimetric plan quality similar as Static-MBRT while maintaining short delivery times of photon-only treatments. This further facilitates integration of pMLC-based MBRT into clinical practice.

Keywords: Mixed-beam radiotherapy, photon multileaf collimator, electron arc therapy

1. Introduction

In external beam radiotherapy, photon treatments performed in clinical routine are typically applied using the photon multileaf collimator (pMLC) integrated into the treatment head of a linear accelerator. The introduction of the pMLC facilitated intensity-modulated radiotherapy (IMRT), which improved target dose conformality compared to 3D conformal radiotherapy (Bortfeld 2006). Volumetric modulated arc therapy (VMAT) has improved upon the delivery efficiency of IMRT while maintaining the dosimetric plan quality by combining synchronized intensity modulation and dynamic gantry rotation (Otto 2008, Teoh et al. 2011).

Meanwhile, standard electron treatments are still applied using patient-specifically fabricated cerrobend cut-outs placed in dedicated electron applicators mounted onto the linear accelerator head for every field and treatment fraction. This makes electron treatments inefficient and cumbersome. Furthermore, using cut-outs for energy modulation or intensity modulation of electron beams is practically infeasible (Hogstrom & Almond 2006). This infeasibility makes electron treatments in inhomogeneous media challenging, where energy modulation is necessary (Asell et al. 1997). Likewise, electron treatments of large targets such as chest wall irradiation are challenging, because multiple conformal electron beams from different directions create hot or cold spots (Khan et al. 1977). To avoid such hot and cold spots, techniques such as electron arc therapy (EAT) have been developed (Khan et al. 1977, Leavitt et al. 1985, McNeely et al. 1988, Leavitt & Stewart 1993, Gaffney et al. 2001, Sharma et al. 2011). In EAT, a narrow electron field is rotated around the patient. Custom secondary collimators are mounted onto the gantry and tertiary collimators, and boli are placed on the patient (Leavitt et al. 1985). The main disadvantage of EAT is that the treatment planning and fabrication and mounting of the custom collimators is very labour and time intensive. More recently, Rodrigues et al. (2014) proposed an EAT technique called dynamic electron arc radiotherapy (DEAR) with a mounted standard applicator and cut-out, reducing the time needed to manufacture custom collimators. To avoid collisions between the applicator and the patient, the table translates synchronously with the gantry rotation. However, an applicator still has to be mounted onto the gantry for every treatment fraction, and dynamic collimation of the beam is not possible. Furthermore, the short distance between the end of the applicator and the patient may increase the collision risk.

To overcome these limitations, some research groups investigated different motorized collimators for electron treatments aiming at replacing the cut-outs and applicators. The investigated collimators were a few leaf electron collimator (FLEC) (Al-Yahya et al. 2005a,b, 2007, Alexander et al. 2010, 2011), a custom electron multileaf collimator (eMLC) (Ma et al. 2000, Gauer et al. 2008, Engel & Gauer 2009, Vatanen et al. 2009, O'Shea et al. 2011, Eldib et al. 2013, Jin et al. 2014), and the existing pMLC (du Plessis et al. 2006, Jin et al. 2008, Asuni et al. 2008, Klein et al. 2008, Salguero et al. 2010, Surucu et al. 2010, Mihaljevic et al. 2011, Henzen et al. 2014a,b, Mueller

et al. 2018a, Fix et al. 2023). Additionally, these motorized collimators make intensity and energy modulation of electron beams feasible in modulated electron radiotherapy (MERT). The pMLC has the additional advantage that no additional hardware needs to be mounted onto the gantry head for every fraction.

However, pMLC collimated electron beams have a larger beam penumbra due to increased scatter within the larger volume of air between the end of the pMLC and the patient (Mueller et al. 2018a). Reducing the source-to-surface distance (SSD) by moving the patient closer to the gantry reduces the beam penumbra. Although, a very short SSD poses a collision risk between the gantry and the patient. It has been shown that electron-only plans do not achieve the same dose homogeneity in the target as photon-only plans (Surucu et al. 2010, Alexander et al. 2011, Henzen et al. 2014b, Mueller et al. 2017, Renaud et al. 2017). A possible solution to overcome these dosimetric limitations of electron beams is to combine electron and photon beams in mixed beam radiotherapy (MBRT) (Li et al. 2000, Korevaar et al. 2002, Mu et al. 2004, Xiong et al. 2004, Palma et al. 2012, Rosca 2012, Renaud et al. 2017, Míguez et al. 2017, Mueller et al. 2017, 2018a, Renaud et al. 2019, Heath et al. 2021, Heng et al. 2021). Mueller et al. (2017) showed that pMLC-based intensity-modulated electron beams combined with static photon beams or photon beams with dynamic trajectories (Mueller et al. 2018b) improved dosimetric plan quality compared to photon-only treatments. However, until now MBRT only contains electron beams delivered from a static gantry angle (Static-MBRT), which results in substantially longer delivery times for Static-MBRT plans compared to VMAT. Besides less patient throughput, longer delivery times might also increase the intrafraction motion and impact patient comfort negatively. We hypothesize that using electron beams with a dynamic gantry rotation during beam-on combined with photon beams (Arc-MBRT) improves the delivery efficiency and thus further facilitates clinical implementation of mixed photon-electron beam treatments.

The aim of this work is to develop a treatment planning process (TPP) to create Arc-MBRT plans consisting of both photon and electron beams with dynamic gantry rotation and pMLC sliding window-based intensity modulation. Several breast cases are investigated retrospectively to demonstrate the delivery efficiency, dosimetric accuracy, and dosimetric plan quality of Arc-MBRT.

2. Methods

An existing TPP used for creating Static-MBRT plans (Mueller et al. 2017, 2022) was extended to accommodate electron beams with a dynamic gantry rotation and sliding window-based intensity modulation, called electron arcs henceforth. The TPP is described in the following subsection. The second subsection describes the investigations of the TPP for Arc-MBRT and describes the dosimetric validation of Arc-MBRT plans.

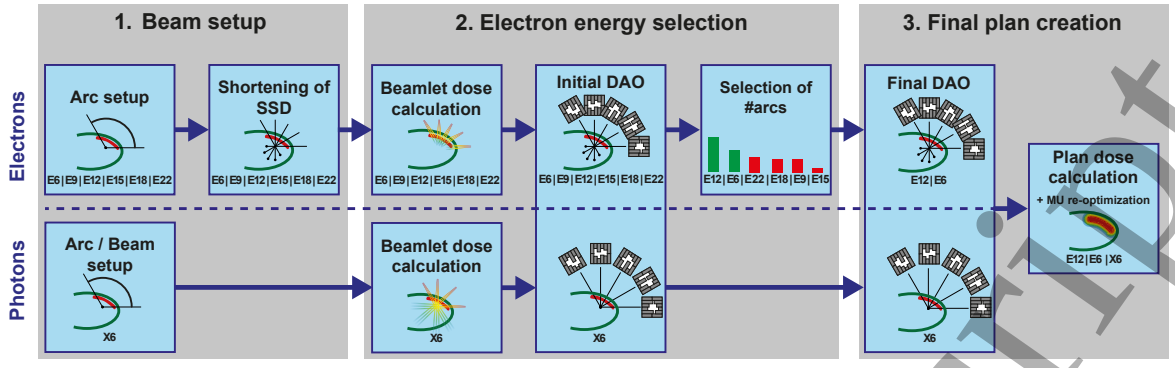

Figure 1. Illustration of the treatment planning process to create Arc-MBRT plans. The upper half describes the steps for the electron beams, while the steps for the photon beams are described in the lower half. SSD: source-surface distance. DAO: direct aperture optimization. Eβ: Electron arc with an energy of β MeV. X6: 6 MV photon arc / beam. MU: Monitor unit.

2.1. Treatment planning process

2.1.1. Beam setup The first part in the TPP illustrated in figure 1 consists of the manual setup of electron arcs and setup of photon beams within a research version of Eclipse. This research version is embedded in the Aria framework v15.6 (Varian Medical Systems, Palo Alto, CA). The user needs to define the gantry range, collimator and table rotation angle for electron arcs. Due to the finite range of electron beams, the gantry range for the electron arcs is suggested to be set to the area where the planning target volume (PTV) is close to the patient's surface. For the defined gantry range, electron arcs are set up for all available electron beam energies with control points (CPs) every 5°. Additionally, the user defines photon beams, consisting either of 3D conformal or intensity-modulated photon beams with a static gantry angle or photon arcs with dynamic gantry rotation (with CPs every 5°). The beams with static gantry angle are called static beams from now on.

Next, the position of the isocenter is shifted for every CP of the electron arcs along the central axis such that the SSD matches a user defined setting $\mathrm{SSD}_{desired}$. This allows to shorten the distance between the gantry head and the patients' surface, which influences the amount of in-air scatter of the electron beams. A shorter SSD hence means a smaller beam penumbra for the electron beams. For this, the current SSD along the central axis $\mathrm{SSD}_{current}$ is calculated and the position of the isocenter is shifted $\Delta_{lateral}$, $\Delta_{vertical}$, and $\Delta_{longitudinal}$ cm along the central beam direction for every CP to match $\mathrm{SSD}_{desired}$. The central beam direction is defined by the the gantry rotation angle α_{gantry} and table rotation angle α_{table} of the CP. The isocenter shift is calculated using the following equations:

$$\Delta_{lateral} = (\mathrm{SSD}_{desired} - \mathrm{SSD}_{current}) \cdot \sin(-\alpha_{gantry}) \cdot \cos(\alpha_{table}) \quad (1)$$

$$\Delta_{vertical} = (\mathrm{SSD}_{desired} - \mathrm{SSD}_{current}) \cdot \cos(\alpha_{gantry}) \quad (2)$$

$$\Delta_{longitudinal} = (\mathrm{SSD}_{desired} - \mathrm{SSD}_{current}) \cdot \sin(-\alpha_{gantry}) \cdot \sin(\alpha_{table}) \quad (3)$$

This results in a dynamic table translation synchronous with the gantry rotation to keep the fixed SSD along the central axis for the electron arcs.

2.1.2. Electron energy selection In the second part of the TPP, the number of electron arcs is reduced to a user-defined number to control the number of total electron arcs in the plan. Because an electron arc was set up for each available beam energy, the delivery time would be unnecessarily long if all electron arcs are used. Thus, the most important electron beam energies are selected based on an initial intensity modulation optimization of all electron arcs and photon beams. For this, a beamlet dose calculation is performed for every CP of electron and photon arcs and static beam using the Eclipse research version interfaced Swiss Monte Carlo Plan (SMCP) (Fix et al. 2007). In SMCP, pre-simulated beamlet phase spaces and the Macro Monte Carlo (MMC) (Neuenschwander et al. 1995, Fix et al. 2013) and Voxel Monte Carlo (VMC++) (Kawrakow & Fippel 2000) dose calculation algorithms are used for electron and photon beams, respectively. The beamlet size is 0.5 cm × 0.5 cm or 0.5 cm × 1 cm in the isocenter plane, depending on the width of the pMLC leaf. For static conformal photon beams, a dose calculation of the whole beam is performed using VMC++. The beamlet dose distributions are then used for the intensity modulation optimization based on a hybrid direct aperture optimization (H-DAO) (Mueller et al. 2022). In H-DAO, apertures describing the pMLC shapes and monitor unit (MU) weights are determined using a hybrid column generation and simulated annealing approach. With column generation, apertures are iteratively generated and with simulated annealing, the shapes and MU weights of the apertures are refined after each aperture addition. For each CP of electron and photon arcs, exactly one aperture is determined, while for static beams a user defined number of apertures is generated. For static conformal photon beams, no apertures are generated, but the MU weight of the static conformal photon beam is simultaneously optimized with the MU weights of the apertures of the electron arcs. The optimization is finished when every CP has exactly one aperture and the static beams have their total number of apertures assigned. For all arcs, the movement range of the pMLC leaves is restricted such that the gantry rotation is not slowed down by the leaf movement and the MU weight is restricted such that the gantry rotation is maximally slowed down to half the full speed. During the optimization, the fluence belonging to an electron or photon aperture is interpolated between consequent CPs as described by Guyer et al. (2022) to account for the continuous movement of the pMLC leaves. For photons, the transmission through the pMLC is considered during the optimization, while for the electrons it is assumed that the transmission through the pMLC is zero due to the thickness of the pMLC.

After the initial DAO, the dose contribution of each electron arc to the PTV is calculated. The electron arcs are then ranked according to their PTV dose contribution from highest to lowest. Only the highest-ranking electron arcs, up to the user-defined number, are kept while the others are discarded.

2.1.3. Final plan creation In the third part, a final DAO is performed with the remaining electron arcs and the photon beams. After all apertures are determined, a dose calculation is performed for each aperture using the SMCP framework (Fix et al. 2007, Manser et al. 2019) considering the exact geometry of the pMLC and the full dynamic movement of the pMLC, table and gantry between consecutive CPs for photon and electron arcs. The source for the electron beams is a validated multiple source model (Henzen et al. 2014a, Fix et al. 2023), consisting of a primary and a jaw source and the dose is calculated using the MMC algorithm. The source of the photon beams is a pre-simulated phase-space located on a plane above the secondary collimator jaws and the dose is calculated using the VMC++ algorithm. After the dose calculation, a MU weight reoptimization is performed to mitigate the differences between the beamlet-based and final dose distributions. Finally, the dose from all apertures is summed to get the plan dose. All dose distributions in this work use a voxel size of $2.5 \times 2.5 \times 2.5\ mm^3$ and the mean statistical uncertainty of the dose in voxels receiving at least 50% of the maximum dose is less than 0.5%.

2.2. Treatment plan investigations

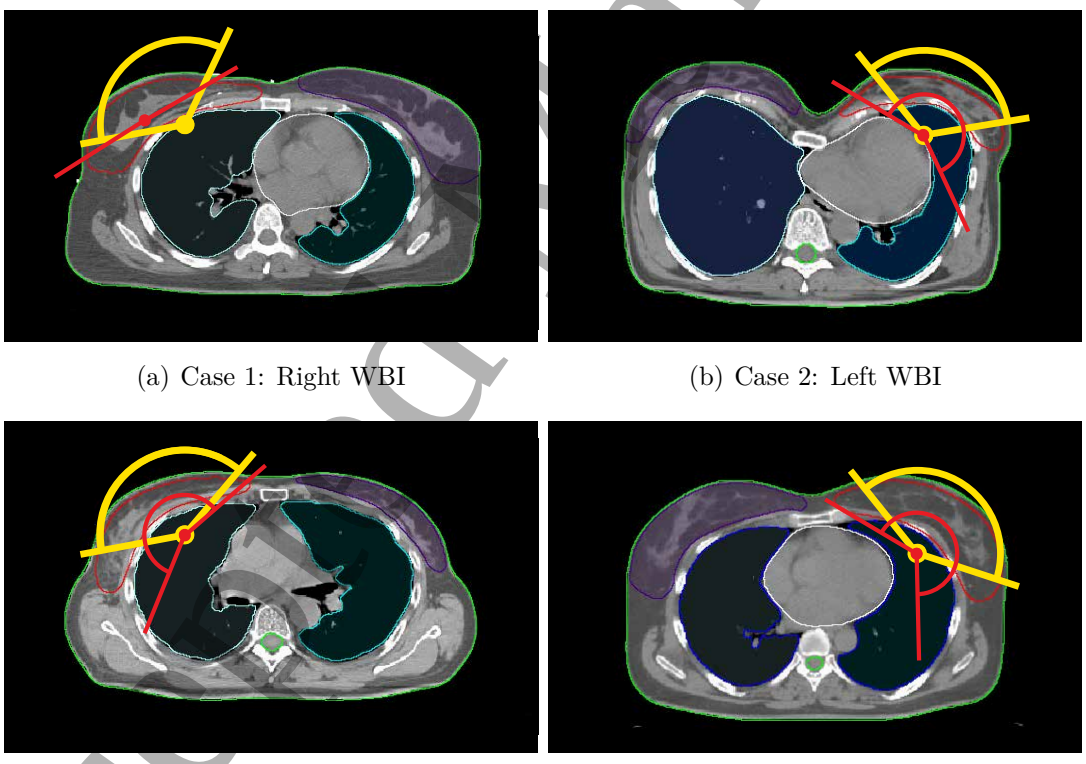

(a) Case 1: Right WBI (b) Case 2: Left WBI

(c) Case 3: Right WBI+LNI (d) Case 4: Left WBI+LNI

Figure 2. Illustration of the beam setup of the Arc-MBRT plans for the four cases. The gantry angle range of the electron arcs is indicated in yellow and the static gantry angles (a) and gantry angle ranges (b, c, d) of the photon beams are indicated in red. WBI: whole breast irradiation. LNI: lymph node irradiation

Four breast cases were selected for retrospective investigation, each with a prescribed total dose of 42.4 Gy to the median dose in the planning target volume (PTV) in 16 fractions. One case is a right-sided whole breast irradiation (WBI) case without axillary lymph node irradiation (LNI), which was clinically treated with 3D conformal radiotherapy (CRT) using two tangential photon beams (case 1). One case is a left-sided WBI case without axillary LNI (case 2), one case is a right-sided WBI case including axillary LNI (case 3) and one case is a left-sided WBI case including axillary LNI (case 4). The cases were selected for the following purposes:

(i) To investigate the influence of the number of electron arcs on the resulting plan.

(ii) To evaluate the dosimetric plan quality and delivery time of Arc-MBRT for breast treatments compared to Static-MBRT and photon-only treatments.

(iii) To validate the deliverability of Arc-MBRT plans in terms of dosimetric accuracy.

Table 1. Beam setup for the Arc-MBRT plans used for investigation of the influence of the number of electron arcs on the resulting treatment plan. The table rotation angle is 0° for all beams. Split beam refers to splitting the beam size using the x-jaws.

	Beam	Gantry angle (°)	Collimator angle (°)
Case 1: Right WBI	2 static conformal photon beams	-123 and 60	102 and 75
	1 – 6 electron arcs	-100 – 30	0
Case 2: Left WBI	2 photon arcs (split beam)	-60 – 155	355
	2 photon arcs (split beam)	-60 – 155	95
	1 – 6 electron arcs	-40 – 80	0
Case 3: Right WBI+LNI	2 photon arcs (split beam)	-155 – 50	355
	2 photon arcs (split beam)	-155 – 50	95
	1 – 6 electron arcs	-100 – 40	0
Case 4: Left WBI+LNI	2 photon arcs (split beam)	-60 –180	355
	2 photon arcs (split beam)	-60 –180	95
	1 – 6 electron arcs	-40 – 110	0

For the first purpose, six Arc-MBRT plans are created for each of the four cases. The six Arc-MBRT plans have a varying number of electron arcs, ranging from 1 to 6 arcs. A plan with 1 electron arc means, that only one electron beam energy is used while a plan with 6 electron arcs means, that all electron beam energies are used, and no arcs were discarded in the electron arcs selection step. The available electron beam energies are 6, 9, 12, 15, 18, and 22 MeV. For all electron arcs, the SSD is shortened to 80 cm as a compromise between reducing the in-air scatter and ensuring collision-free delivery (Mueller et al. 2018a, Ma et al. 2019). The photon beam setup for case 1 (right WBI) consists of two static conformal tangential beams and of four partial VMAT arcs for the other three cases. The beam setups are illustrated in figure 2 and described in detail in table 1. For all plans, the dose contribution to the PTV of the electron and photon beams is investigated and the dosimetric plan quality of the plans with 2 and 6 electron arcs are analyzed in detail.

Table 2. Beam setup for the plans used for investigating the dosimetric plan quality of Arc-MBRT. In brackets, the gantry ranges and gantry angles of the photon and electron beams are indicated. The table angle is 0° for all beams. The photon arcs are always split beams using the x-jaws.

	Plan (electrons | photons)	Electron beams	Photon beams
Case 1: Right WBI	Arc-MBRT (2 arcs | 2 static conf)	2 arcs (-100° – 30°)	2 static conformal (-123° & 60°)
	Static-MBRT (3 static | 2 static conf)	3 static (-80°, -35° and 0°)	2 static conformal (-123° & 60°)
	CRT (0 | 2 static conf)	–	2 static conformal (-123° & 60°)
	Arc-MBRT (2 arcs | 2 static)	2 arcs (-100° – 30°)	2 static (-123° & 60°)
	Static-MBRT (3 static | 2 static)	3 static (-80°, -35° and 0°)	2 static (-123° & 60°)
	IMRT (0 | 2 static)	–	2 static (-123° & 60°)
	Arc-MBRT (2 arcs | 2 arcs)	2 arcs (-100° – 30°)	2 arcs (-160° – 60°)
	Static-MBRT (3 static | 2 arcs)	3 static (-80°, -35° and 0°)	2 arcs (-160° – 60°)
	VMAT (0 | 4 arcs)	–	4 arcs (-160° – 60°)
Case 2: Left WBI	Arc-MBRT (2 arcs | 4 arcs)	2 arcs (-40° – 80°)	4 arcs (-60° – 155°)
	Static-MBRT (3 static | 4 arcs)	3 static (-30°, 28° and 63°)	4 arcs (-60° – 155°)
	VMAT (0 | 6 arcs)	–	6 arcs (-60° – 155°)
Case 3: Right WBI+LNI	Arc-MBRT (2 arcs | 4 arcs)	2 arcs (-100° – 40°)	4 arcs (-155° – 50°)
	Static-MBRT (3 static | 4 arcs)	3 static (-76° - 46° and 0°)	4 arcs (-155° – 50°)
	VMAT (0 | 6 arcs)	–	6 arcs (-155° – 50°)
Case 4: Left WBI+LNI	Arc-MBRT (2 arcs | 4 arcs)	2 arcs (-40° – 110°)	4 arcs (-60° – 180°)
	Static-MBRT (3 static | 4 arcs)	3 static (-25°, 33° and 79°)	4 arcs (-60° – 180°)
	VMAT (0 | 6 arcs)	–	6 arcs (-60° – 180°)

For the second purpose, Arc-MBRT plans, Static-MBRT plans, and photon-only plans are created and the dosimetric plan quality and the estimated delivery time is compared for all plans of the four cases. The different plans are described in detail in table 2. All electron arcs and static electron beams have an SSD of 80 cm. Comparisons between the dosimetric plan quality of the resulting plans is performed by analyzing dose-volume histogram (DVH) parameters for the PTV, heart, lung, contralateral breast and spinal canal. For the PTV, the Paddick conformity index (CI) (Paddick 2000) and homogeneity index (HI = $(D_{2\%} - D_{98\%})/D_{50\%}$) are calculated and compared, where $D_{X\%}$ represents the minimum dose in $X\%$ of the PTV volume. The estimated delivery times are calculated by summing the time per CPs of all arcs and beams of one plan, while the accelerations of the mechanical axes are neglected. Additionally, the time to move all axes to the starting position of the next arc / beam is taken into account with a minimum time of 20 s for switching between photon and electron beams and between different electron energies.

For the third purpose, the Arc-MBRT plans for the left WBI and right WBI+LNI cases (cases 2 & 3) are delivered on a TrueBeam linear accelerator (Varian Medical Systems) equipped with a Millennium 120 pMLC (Varian Medical Systems) in developer mode. The dose is measured using radiochromic EBT3 film sheets (Ashland Advanced Materials, Bridgewater, NJ) placed in 1 cm depth inside a PMMA cube. Film measurements are taken for each plan for the following deliveries:

(i) The total plan (each consisting of two electron and four photon arcs).

(ii) Only the electron arcs of each plan.

(iii) The electron arcs with a collapsed gantry angle to 0°.

The reason for these different deliveries is to measure individually the dosimetric accuracy of the whole plan, of the electron arcs and the sliding window technique for electrons. The film sheets are scanned using an Epson XL 10000 flatbed scanner (Seiko Epson Co., Tokyo, Japan) 18h after irradiation. The scanned films are corrected for the lateral response artifact of the scanner using a one-dimensional linear correction function (Lewis & Chan 2015), converted to absolute dose using a triple channel calibration (Micke et al. 2011) and rescaled according to the one-scan protocol by using two additional film strips (Lewis et al. 2012). The resulting dose distribution of the red channel is compared to the corresponding 2D plane of the dose recalculated for the PMMA cube using a gamma evaluation with a 3% (global) / 2 mm criterion and a 10% low-dose threshold of the maximum dose.

3. Results

3.1. Number of electron arcs

The dose contributions to the PTV of the different electron and photon beams in Arc-MBRT plans varying in the number of electron arcs are shown in figure 3 for the four cases. For case 1 (right WBI), the electron dose contribution increases from 31% to 51% with increasing number of electron arcs. For case 2 (left WBI), the electron dose contribution is between 13% and 19% for all six plans. The electron dose contribution for case 3 (right WBI+LNI) increases from 11% to 29% from one to six electron arcs. Similarly, the electron dose contribution for the Left WBI+LNI case increases from 16% to 28% from one to six electron arcs. The electron dose contribution is almost twice as high in case 1 (right WBI) compared to all other cases. Overall, the lower three electron energies contribute more than half of the electron dose contribution for all four cases.

In figure 4, the DVHs of Arc-MBRT plans with 2 and 6 electron arcs are shown. For case 1 (right WBI), the maximum dose to the ipsilateral lung slightly decreases while the low-dose bath to the lung slightly increases from 2 to 6 electron arcs. The PTV coverage and dose to the OARs are similar for case 2 (left WBI). The two-electron arc plan of case 3 (right WBI+LNI) has a higher maximum dose to the spinal canal and a slightly increased mean dose to the contralateral lung while maintaining the same PTV coverage as the six-electron arc plan. For case 4 (left WBI+LNI), the PTV coverage and dose to OARs is similar between the 2 and 6 electron arc plans. Overall, the dosimetric plan quality is similar between the two plans for each of the four cases.

3.2. Dosimetric investigations

3.2.1. Case 1: Right WBI The results of the dosimetric comparison for case 1 (right WBI) are shown in figure 5. The dosimetric values and estimated delivery times are presented in table 3. The MBRT plans with static conformal photon beams have a reduced PTV coverage in comparison with the CRT plan. On the other hand, the volume of normal tissue receiving 100% of the prescribed dose is reduced in the MBRT

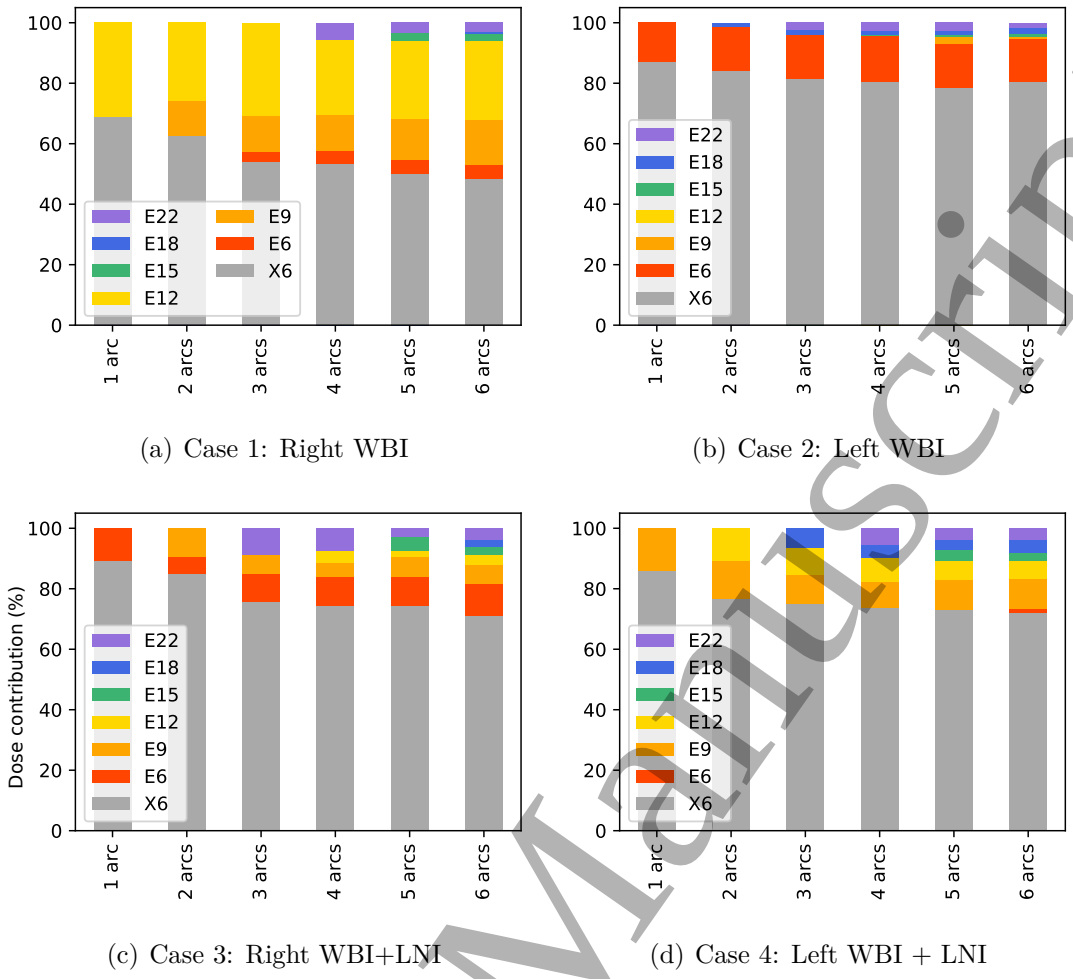

(a) Case 1: Right WBI

(b) Case 2: Left WBI

(c) Case 3: Right WBI+LNI

(d) Case 4: Left WBI + LNI

Figure 3. Dose contribution to the PTV of electron and photon beams in Arc-MBRT plans with the number of electron arcs ranging from 1 to 6 arcs for all four cases. Eβ: Electron arc with an energy of β MeV. X6: VMAT arc with 6 MV photons.

plans compared with the CRT plan. For the MBRT plans with static photon beams and MBRT plans with photon arcs, the PTV coverage is similar to the IMRT plan and VMAT plan, respectively, while the dose to the normal tissue is reduced in the MBRT plans.

Comparing Arc-MBRT plans versus Static-MBRT plans, the delivery time is reduced by at least 55%. The estimated delivery time of the photon-only plans is 35% and 16% shorter for the CRT and IMRT plans and 37% longer for the VMAT plan compared to the respective Arc-MBRT plans.

3.2.2. Case 2: Left WBI The Arc-MBRT, Static-MBRT and VMAT plans for case 2 (left WBI) are compared in figure 6 (dose distributions and DVHs) and in table 4 (dosimetric values & delivery time). As can be seen in the top of figure 6, the electron dose contributes mostly to the superficial part of the PTV and to the part where the heart is close to the PTV in the distal direction. The photon dose covers the more

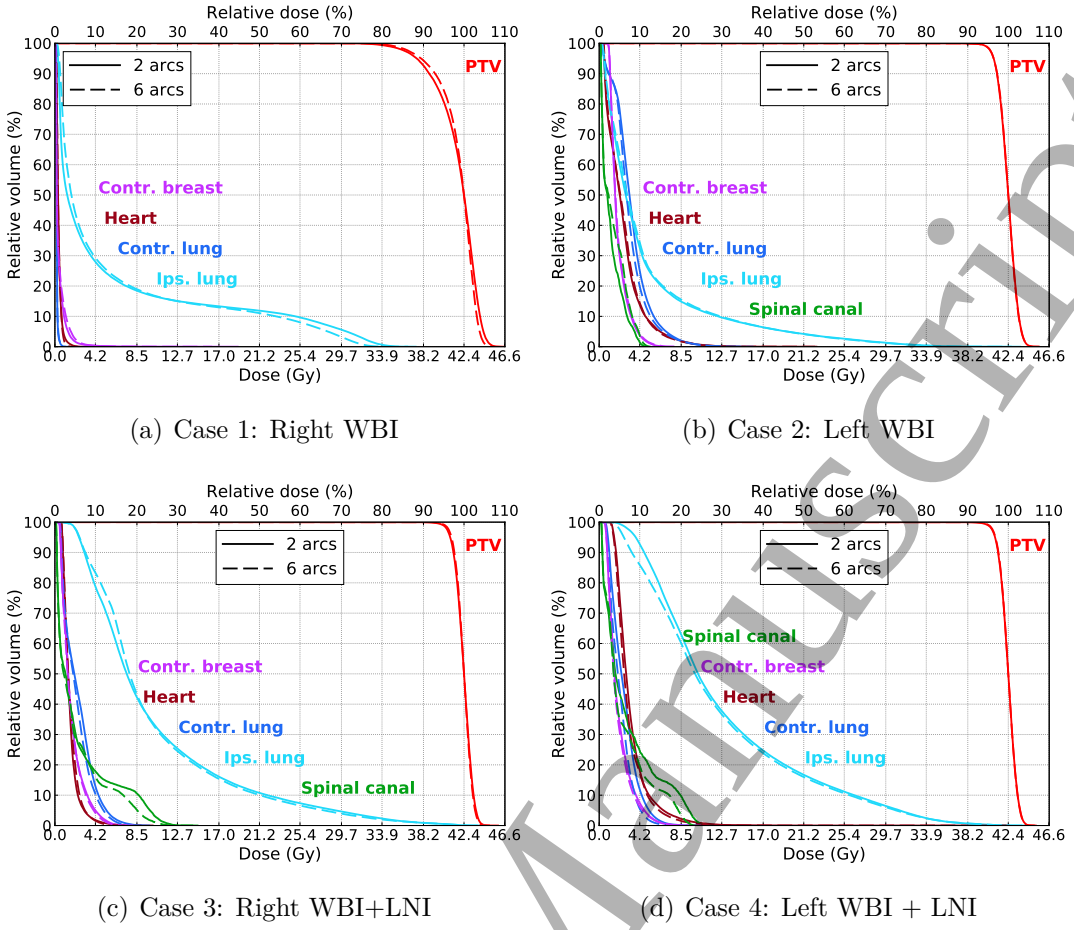

(a) Case 1: Right WBI

(b) Case 2: Left WBI

(c) Case 3: Right WBI+LNI

(d) Case 4: Left WBI + LNI

Figure 4. DVH comparisons of Arc-MBRT plans with 2 and 6 electron arcs for each of the four cases.

distal parts of the PTV, especially near the ribs where the ipsilateral lung is only a few millimeters apart from the PTV.

While the PTV coverage and the dose to OARs are similar in the Arc-MBRT and Static-MBRT plans, the dose to the OARs is substantially higher in the photon-only VMAT plan. Compared to the VMAT plan, the mean dose to the heart is reduced by 32%, the mean dose to the contralateral breast is reduced by 23% and the V_{5Gy} of the total lung is reduced by 40% in the Arc-MBRT plan.

3.2.3. Cases 3&4: Left and right WBI+LNI The DVH comparison of the Arc-MBRT, Static-MBRT and VMAT plans for cases 3 and 4 (right and left WBI+LNI) are shown in figure 7. In table 5, the dosimetric values and delivery times for case 3 (right WBI+LNI) are compared and the dosimetric values and delivery times for case 4 (left WBI+LNI) are compared in table 6.

In case 3 (right WBI+LNI), the Arc-MBRT and Static-MBRT achieved similar dosimetric plan quality. Both plans have a similar PTV coverage as the VMAT plan. When comparing the Arc-MBRT plan to the VMAT plan, the mean dose to the heart

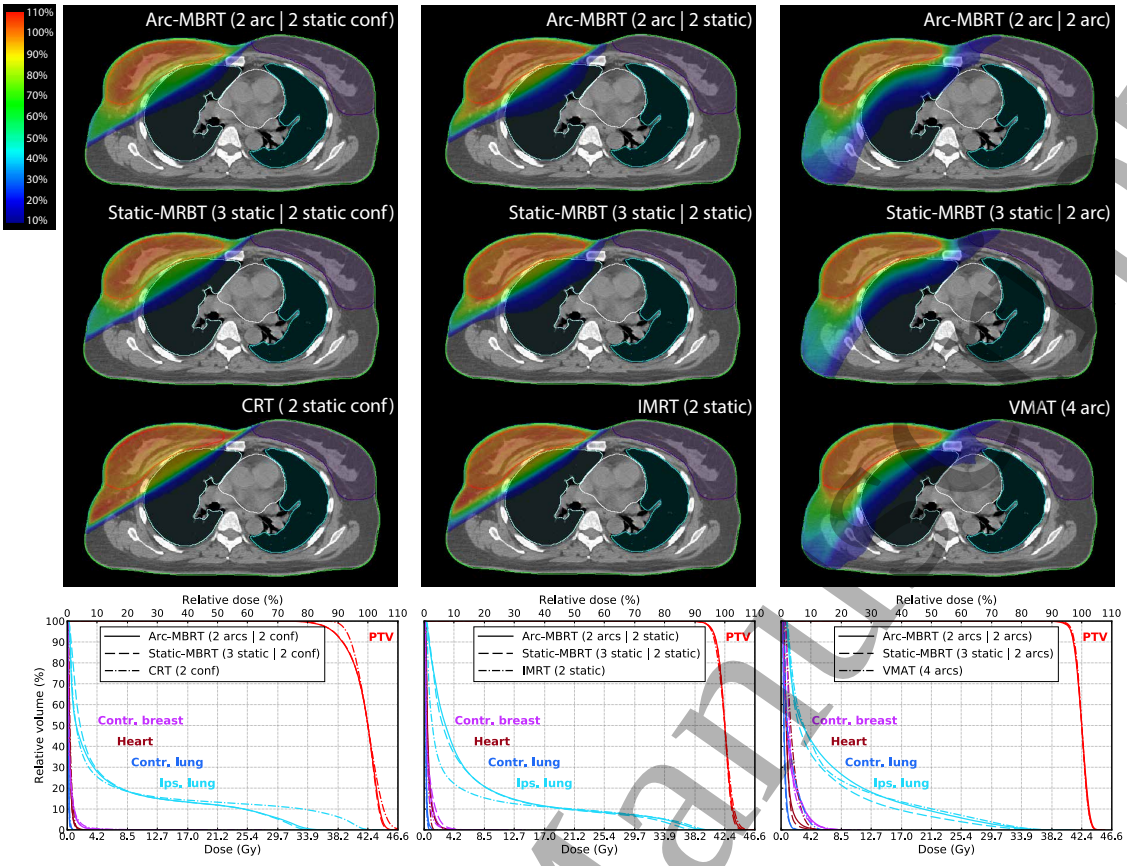

Figure 5. Dose color wash comparison (top) on a representative transversal plane and DVH comparison (bottom) of the Arc-MBRT, Static-MBRT and photon-only plans for case 1 (right WBI). To distinguish between the different photon beam setups, the electron and photon beams are indicated in brackets.

is reduced by 60%. Similarly, the mean dose to the contralateral breast is reduced by 51% and the V_{5Gy} of the total lung is reduced by 24%.

The Arc-MBRT and Static-MBRT plans for case 4 (left WBI+LNI) have similar dosimetric plan quality, except for the lung, which has a lower dose bath in the Static-MBRT plan compared to the Arc-MBRT plan. The VMAT plan has the same PTV coverage as both MBRT plans, but the mean dose to the heart is reduced by 38%, the mean dose to the contralateral breast is reduced by 23% and the V_{5Gy} of the total lung is reduced by 15% in the MBRT plans compared to the VMAT plan.

3.3. Dosimetric validation

The Arc-MBRT plans for case 2 (left WBI) and case 3 (right WBI+LNI) case were successfully delivered on a TrueBeam and film measurements were taken for the total plans (one fraction), only the electron arcs of each plan and the electron arcs of each plan with a collapsed gantry angle to 0°. The results of the comparisons between the measured and calculated dose distributions for all six deliveries are shown in figure 8. The gamma analysis for case 2 (left WBI) resulted in a passing rate of 98.5% for the

Table 3. Comparison of the dosimetric quantities of the Arc-MBRT, Static-MBRT and photon-only plans for case 1 (right WBI). The best value of each quantity whithin the group is highlighted in bold.

	Arc-MBRT	Static-MBRT	photon-only RT
	(2 arcs | 2 static conf)	(3 static | 2 static conf)	(2 static conf)
HI (%)	21	20	**17**
CI	**0.50**	0.49	0.33
Normal tissue $V_{42.4Gy}$ (cm^3)	**2**	**2**	136
Heart D_{mean} (Gy)	**0.4**	**0.4**	**0.4**
Contr. breast D_{mean} (Gy)	**0.4**	**0.4**	**0.4**
Ips. lung V_{17Gy} (%)	**13.3**	**13.3**	14.2
Ips. lung $D_{2\%}$ (Gy)	32.5	**31.8**	40.7
Estimated delivery time (min)	2.3	8.5	**1.5**
Electron dose contribution (%)	37	40	–
	(2 arcs | 2 static)	(3 static | 2 static)	(2 static)
HI (%)	10	**9**	11
CI	**0.50**	0.49	0.40
Normal tissue $V_{42.4Gy}$ (cm^3)	5	**1**	78
Heart D_{mean} (Gy)	0.6	0.6	**0.5**
Contr. breast D_{mean} (Gy)	0.6	0.6	**0.5**
Ips. lung V_{17Gy} (%)	11.4	11.2	**11.1**
Estimated delivery time (min)	5.7	12.6	**4.8**
Electron dose contribution (%)	35	50	–
	(2 arcs | 2 arcs)	(3 static | 2 arcs)	(4 arcs)
HI (%)	8	8	**7**
CI	**0.50**	**0.50**	0.49
Normal tissue $V_{42.4Gy}$ (cm^3)	**2**	3	21
Heart D_{mean} (Gy)	**0.8**	**0.8**	1.6
Contr. breast D_{mean} (Gy)	**1.3**	1.4	1.5
Ips. lung V_{17Gy} (%)	12.8	**9.4**	13.4
Estimated delivery time (min)	**3.0**	7.8	4.1
Electron dose contribution (%)	41	37	–

total dose, 99.5% for the electron dose and 100% for the collapsed dose, respectively. The passing rates of case 3 (right WBI+LNI) were 100% for all three dose distributions.

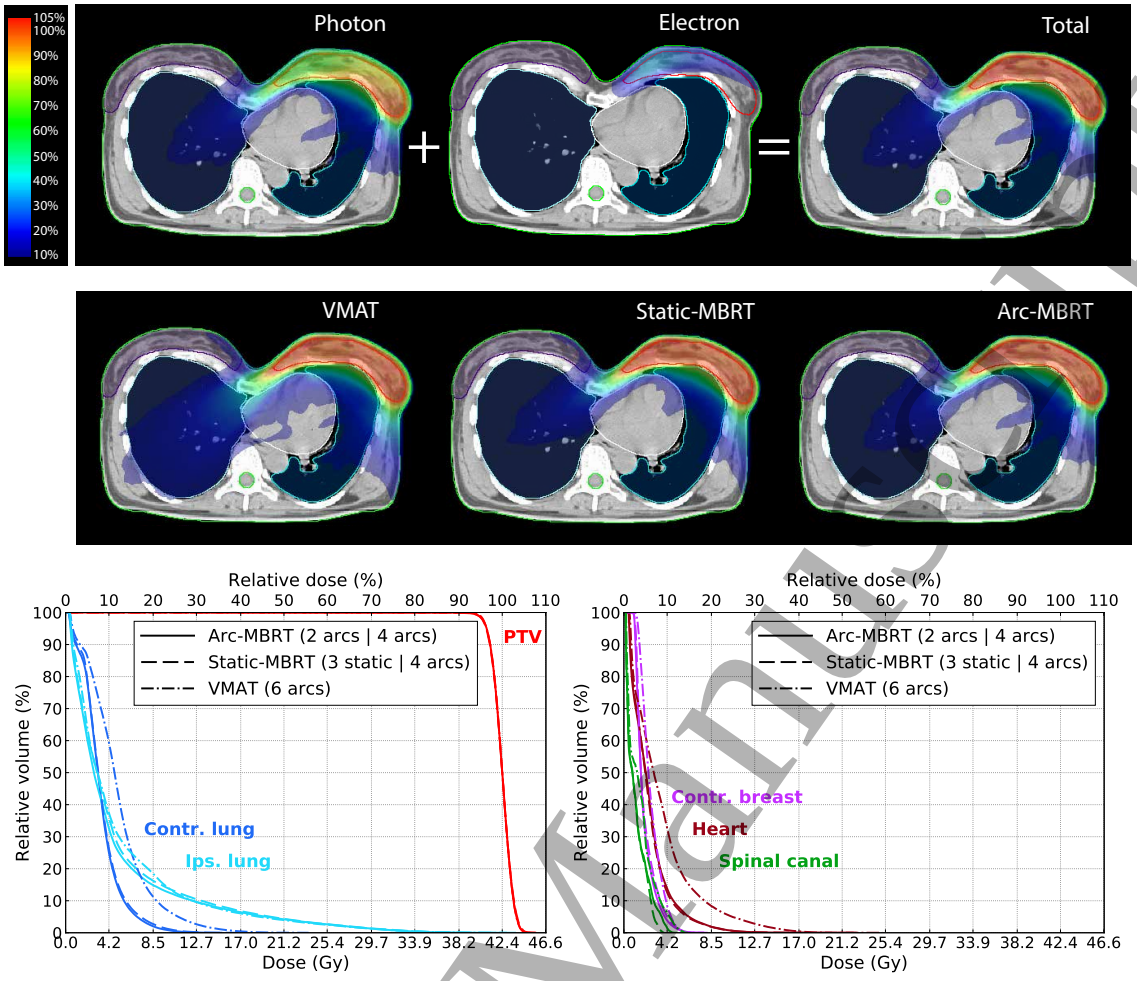

Figure 6. Dose color wash comparison (top) on a representative transversal plane between the photon and electron dose contributions of the Arc-MBRT plan, dose color wash comparison (middle) and DVH comparison (bottom) of the Arc-MBRT, Static-MBRT and VMAT plans for case 2 (left WBI).

Table 4. Comparison of the dosimetric quantities of the Arc-MBRT, Static-MBRT and VMAT plans for case 2 (left WBI). The best value of each quantity is highlighted in bold.

	Arc-MBRT	Static-MBRT	VMAT
HI (%)	8.5	8.8	**8.4**
CI	**0.50**	0.49	0.49
Heart D_{mean} (Gy)	**2.5**	**2.5**	3.7
Contr. breast D_{mean} (Gy)	**2.0**	2.1	2.6
Ips. lung V_{17Gy} (%)	6.4	6.8	**6.0**
Total lung V_{5Gy} (%)	**19.2**	20.6	39.6
Spinal canal $D_{2\%}$ (Gy)	4.1	**3.3**	5.0
Normal tissue $V_{10\%}$ (%)	**10.9**	11.6	16.5
Estimated delivery time (min)	**4.4**	8.9	5.3
Electron dose contribution (%)	16	15	–

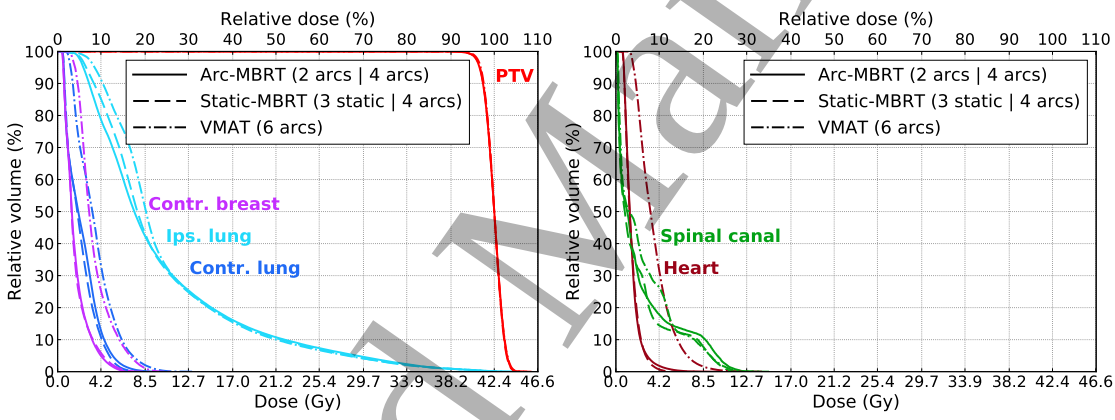

(a) Case 3: Right WBI+LNI

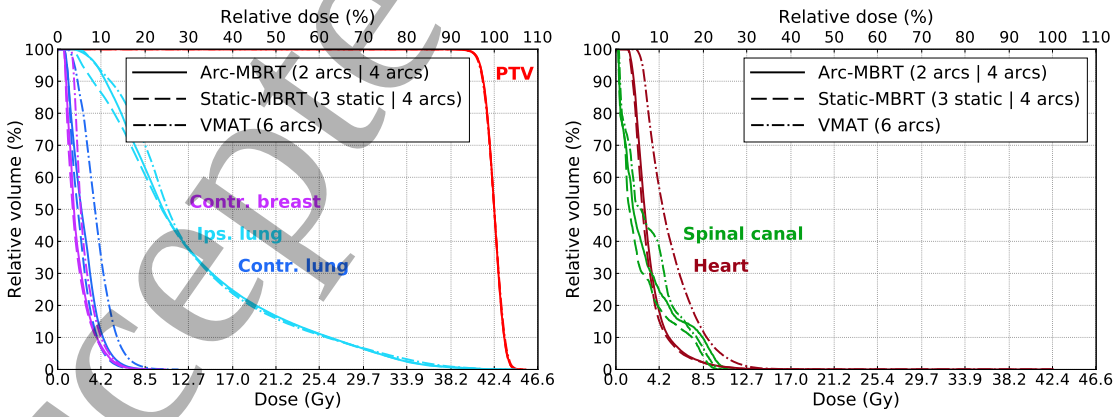

(b) Case 4: Left WBI+LNI

Figure 7. DVH comparison of the Arc-MBRT, Static-MBRT and VMAT plans for case 3 (a) and case 4 (b).

Table 5. Comparison of the dosimetric quantities of the Arc-MBRT, Static-MBRT and VMAT plans for case 3 (right WBI+LNI). The best value of each quantity is highlighted in bold.

	Arc-MBRT	Static-MBRT	VMAT
HI (%)	7.9	7.8	**7.7**
CI	**0.50**	**0.50**	**0.50**
Heart D_{mean} (Gy)	**1.5**	**1.5**	3.8
Contr. breast D_{mean} (Gy)	**1.7**	**1.7**	3.5
Ips. lung V_{17Gy} (%)	16.1	15.8	**15.4**
Total lung V_{5Gy} (%)	**43.2**	45.8	56.8
Spinal canal $D_{2\%}$ (Gy)	10.6	**10.1**	10.3
Normal tissue $V_{10\%}$ (%)	22.7	**21.5**	27.9
Estimated delivery time (min)	4.4	10.3	**4.1**
Electron dose contribution (%)	15	25	–

Table 6. Comparison of the dosimetric quantities of the Arc-MBRT, Static-MBRT and VMAT plans for case 4 (left WBI+LNI). The best value of each quantity is highlighted in bold.

	Arc-MBRT	Static-MBRT	VMAT
HI (%)	**7.6**	**7.6**	8.0
CI	**0.50**	**0.50**	**0.50**
Heart D_{mean} (Gy)	3.3	**3.1**	5.3
Contr. breast D_{mean} (Gy)	**2.0**	**2.0**	2.6
Ips. lung V_{17Gy} (%)	24.7	24.3	**23.7**
Total lung V_{5Gy} (%)	46.2	**42.4**	54.6
Spinal canal $D_{2\%}$ (Gy)	9.9	**8.9**	9.4
Normal tissue $V_{10\%}$ (%)	29.3	**26.0**	34.3
Estimated delivery time (min)	4.7	9.8	**4.6**
Electron dose contribution (%)	24	29	–

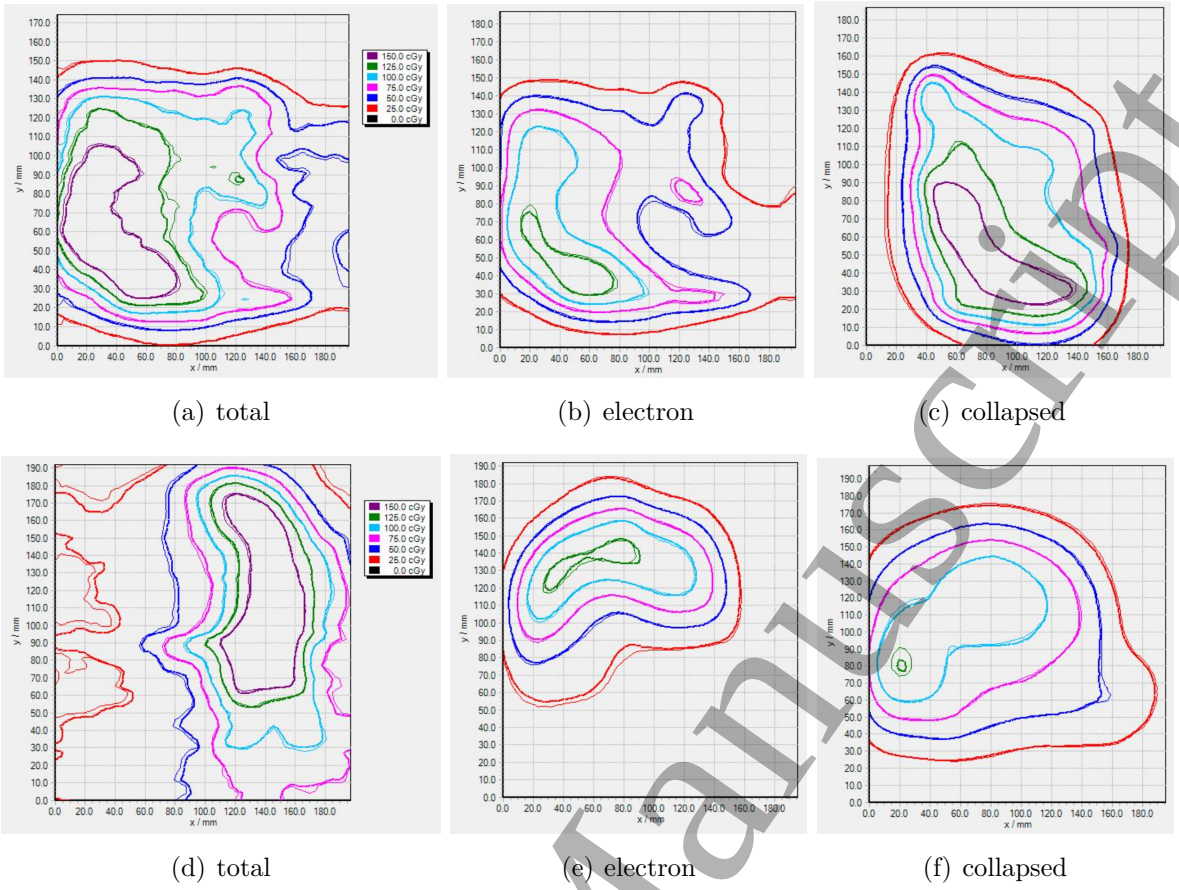

(a) total (b) electron (c) collapsed

(d) total (e) electron (f) collapsed

Figure 8. Measured (thin) and calculated (thick) isodose lines for dose distributions of case 2 (top) and case 3 (bottom). In a) and d) the total Arc-MBRT plans consisting of electron and photon arcs were delivered, in b) and e) the electron arcs were delivered with dynamic gantry and table and in c) and f) the electron arcs were delivered with a collapsed gantry angle.

4. Discussion

In this work, a TPP for creating Arc-MBRT plans was successfully developed. The Arc-MBRT plans consist of intensity-modulated electron arcs and static or dynamic photon beams. The intensity-modulated electron arcs are achieved with a pMLC-based sliding-window technique and synchronous dynamic gantry rotation and table translation to keep a shortened SSD. In contrast to Static-MBRT, which contains intensity-modulated electron beams delivered from a static gantry angle, the gantry moves continuously during beam-on for electron arcs. This shortens the delivery time substantially. For the four investigated cases, the delivery times of the Arc-MBRT plans are less than half the time of the Static-MBRT plans. This is similar to the advantage of VMAT over IMRT, which also has reduced delivery time due to the dynamic gantry rotation (Teoh et al. 2011). Additionally, creating a suitable beam setup for Static-MBRT plans is not always straightforward. Multiple beams must be chosen carefully to achieve an acceptable coverage of the PTV by the electrons. The presented TPP improves this, as setting up gantry ranges for electron arcs is more straightforward. The TPP presented here can create Arc-MBRT plans, but plans consisting of electron arcs only can also be created with the same TPP in a similar way.

The dosimetric plan quality of Arc-MBRT plans are generally similar to the Static-MBRT but are superior compared to the photon-only treatments, except for the combination of electron arcs with static conformal photon beams. A possible explanation for this is that the dose of the conformal photon beams is predetermined and only the MU weight of the conformal beams can be changed during intensity modulation optimization. This indicates that the simultaneous optimization of photon and electron intensity modulation is important. For all other setups, the mixed beam plans achieved the same PTV coverage while reducing the dose to the OARs. Most notably, MBRT plans reduced the mean dose to the heart compared to photon-only plans, which is correlated with ischemic heart disease (Darby et al. 2013). Similar results were obtained by Li et al. (2000), Al-Yahya et al. (2005b), Alexander et al. (2011), Renaud et al. (2017) using different MBRT techniques. This shows the potential dosimetric superiority of MBRT plans over photon-only treatments for breast cases also for MBRT utilizing intensity modulated electron arcs.

When comparing Arc-MBRT plans with different number of electron arcs, it seemed that for the investigated breast cases no more than two electron arcs are necessary to achieve a good dosimetric plan quality and that more electron arcs only increase the delivery time without improving the dosimetric result substantially. This can be explained by the fact that energy modulation does not play a substantial role for this treatment site, as the range of treatment depths is narrow. Rather, the electron dose acts as a base dose in the superficial parts of the PTV, allowing for a lower photon dose to the OARs while maintaining a sharp dose falloff outside the PTV. In the cases including LNI, the lymph nodes are essentially only covered with photons. Because the lymph nodes are not near the patient's skin, a larger portion of normal tissue would be

irradiated if the electron beams would contribute more to this area and thus only the superficial parts of the PTV in the breast are covered with electrons.

Arc-MBRT plans were successfully delivered on a TrueBeam and the dosimetric validation shows good agreement between the measured and calculated dose distributions. This shows that the multiple-source beam model and algorithm used for the electron dose calculation are suitable for Arc-MBRT plans and that a TrueBeam can deliver electron arcs accurately. Ma et al. (2019) investigated dosimetric characterizations of electron arcs and achieved good agreements between Monte Carlo dose calculations and measurements as well. However, no intensity-modulated electron arcs were measured.

In the presented TPP for Arc-MBRT, the time for dose calculation can be substantially longer compared to the time required for photon-only VMAT plans. There are several approaches possible to reduce this dose computation time. One approach is to use a coarser dose scoring grid to determine suitable electron energies. The number of electron energies for which beamlet dose has to be calculated on the regular dose scoring grid can thus be reduced. Another approach is to use faster dose calculation algorithms based on a GPU implementation (Franciosini et al. 2023) or on deep learning methods for denoising MC dose distributions (Bai et al. 2021, Neph et al. 2021).

One aspect which was not investigated in this work is the robustness of the treatment plans against setup uncertainties and patient breathing. The assumption that the dose distribution is not perturbed by setup uncertainties does not hold for electrons and the electron dose distribution moves with the patient in the incident beam direction (Thomas 2006). Additionally, electron beams might be more robust than photon beams due to their larger beam penumbra. Renaud et al. (2019), Heath et al. (2021) developed a clinical target volume (CTV) based robust optimization approach for Static-MBRT. They showed that robust-optimized plans exhibited less dosimetric impact due to setup uncertainties compared to plans using conventional PTV margins and that the electron dose contribution was higher in the robust-optimized plans. Additionally, it has been shown that also photon-only plans could benefit from CTV-based robust optimization as well (Byrne et al. 2016). Hypothetically, robust-optimized Arc-MBRT would show the same benefit and will be investigated in future research, but the potential burden on computer memory and calculation time of the many MC beamlets needed for robust optimization needs to be addressed adequately (Mueller et al. 2023).

This work focused on breast cases to show the dosimetric plan quality and efficiency of Arc-MBRT plans. However, there is a potential advantage of MBRT also for other treatment sites with a superficial part such as head-and-neck cancers (Mu et al. 2004, Mueller et al. 2018a), brain tumors (Rosca 2012, Heath et al. 2021), sarcomas (Renaud et al. 2017), tumors in the abdomen (Unkelbach et al. 2022) or scalp irradiations (Eldib et al. 2017). Additionally, non-coplanar beam directions for photon and electron beams might offer an additional advantage. Electron beams with dynamic trajectories similar to the dynamic trajectories of photon beams in dynamic mixed beam radiotherapy (Mueller et al. 2018b) might be explored in future research. Although, ensuring collision

avoidance for the shortened SSD might be challenging for non-coplanar electron beams.

5. Conclusion

A TPP for pMLC-based Arc-MBRT containing intensity-modulated electron beams with dynamic gantry rotation was successfully developed. Created Arc-MBRT plans for four breast cases showed similar dosimetric plan quality to Static-MBRT plans while outperforming photon-only plans. For the investigated breast cases, two electron arcs were enough to achieve a good dosimetric plan quality. On average, the mean heart dose is reduced by 32% in the MBRT plans compared to the photon-only plans. The Arc-MBRT plans reduced the delivery time by half compared to Static-MBRT plans and were similar to VMAT plans, which further facilitates integration of pMLC-based mixed-beam radiotherapy into clinical practice.

6. Acknowledgements

This work was supported by grant 200021_185366 of the Swiss National Science Foundation and by Varian Medical Systems. Calculations are performed on ubelix, the high-performance computing cluster at the University of Bern. The data that support the findings of this study are available upon request from the authors.

References

Al-Yahya, K., Hristov, D., Verhaegen, F. & Seuntjens, J. (2005a), 'Monte carlo based modulated electron beam treatment planning using a few-leaf electron collimator a feasibility study', *Phys. Med. Biol.* **50**, 847.

Al-Yahya, K., Schwartz, M., Shenouda, G., Verhaegen, F., Freeman, C. & Seuntjens, J. (2005b), 'Energy modulated electron therapy using a few leaf electron collimator in combination with imrt and 3d-crt: Monte carlo-based planning and dosimetric evaluation', *Med. Phys.* **32**, 2976–2986.

Al-Yahya, K., Verhaegen, F. & Seuntjens, J. (2007), 'Design and dosimetry of a few leaf electron collimator for energy modulated electron therapy', *Med. Phys.* **34**, 4782–4791.

Alexander, A., DeBlois, F. & Seuntjens, J. (2010), 'Toward automatic field selection and planning using monte carlo-based direct aperture optimization in modulated electron radiotherapy', *Phys. Med. Biol.* **55**, 4563–4576.

Alexander, A., Soisson, E., Hijal, T., Sarfehnia, A. & Seuntjens, J. (2011), 'Comparison of modulated electron radiotherapy to conventional electron boost irradiation and volumetric modulated photon arc therapy for treatment of tumour bed boost in breast cancer', *Radiother. Oncol.* **100**, 253–258.

Asell, M., Hyödynmaa, S., Gustafsson, A. & Brahme, A. (1997), 'Optimization of 3d conformal electron beam therapy in inhomogeneous media by concomitant fluence and energy modulation', *Phys. Med. Biol.* **42**(11), 2083.

Asuni, G., Beek, T. A. V., Venkataraman, S., Klein, E. E., Mamalui-Hunter, M. & Low, D. A. (2008), 'Delivery of modulated electron beams with conventional photon multi-leaf collimators', *Phys. Med. Biol.* **54**, 327.

Bai, T., Wang, B., Nguyen, D. & Jiang, S. (2021), 'Deep dose plugin: towards real-time monte carlo dose calculation through a deep learning-based denoising algorithm', *Mach. Learn.: Sci. Technol.* **2**(2), 025033.

Bortfeld, T. (2006), 'Imrt: a review and preview', *Phys. Med. Biol.* **51**, R363.

Byrne, M., Hu, Y. & Archibald-Heeren, B. (2016), 'Evaluation of raystation robust optimisation for superficial target coverage with setup variation in breast imrt', *Australas. Phys. Eng. Sci. Med.* **39**, 705–716.

Darby, S. C., Ewertz, M., McGale, P., Bennet, A. M., Blom-Goldman, U., Brønnum, D., Correa, C., Cutter, D., Gagliardi, G., Gigante, B., Jensen, M.-B., Nisbet, A., Peto, R., Rahimi, K., Taylor, C. & Hall, P. (2013), 'Risk of ischemic heart disease in women after radiotherapy for breast cancer', *N. Engl. J. Med.* **11**, 987–98.

du Plessis, F. C. P., Leal, A., Stathakis, S., Xiong, W. & Ma, C.-M. (2006), 'Characterization of megavoltage electron beams delivered through a photon multi-leaf collimator (pmlc)', *Phys. Med. Biol.* **51**, 2113–2129.

Eldib, A., Jin, L., Li, J. & Ma, C. M. C. (2013), 'Feasibility of replacing patient specific cutouts with a computer-controlled electron multileaf collimator', *Phys. Med. Biol.* **58**, 5653.

Eldib, A., Jin, L., Martin, J., Fan, J., Li, J., Chibani, O., Veltchev, I., Price, R., Galloway, T. & Ma, C.-M. C. (2017), 'Investigating the dosimetric benefits of modulated electron radiation therapy (mert) for partial scalp patients', *Biomed. Phys. Eng. Express* **3**, 035013.

Engel, K. & Gauer, T. (2009), 'A dose optimization method for electron radiotherapy using randomized aperture beams', *Phys. Med. Biol.* **54**, 5253.

Fix, M. K., Cygler, J., Frei, D., Volken, W., Neuenschwander, H., Born, E. J. & Manser, P. (2013), 'Generalized emc implementation for monte carlo dose calculation of electron beams from different machine types', *Phys. Med. Biol.* **58**, 2841–2859.

Fix, M. K., Frei, D., Mueller, S., Guyer, G., Loebner, H. A., Volken, W. & Manser, P. (2023), 'Auto-commissioning of a monte carlo electron beam model with application to photon mlc shaped electron fields', *Phys. Med. Biol.* .

Fix, M. K., Manser, P., Frei, D., Volken, W., Mini, R. & Born, E. J. (2007), 'An efficient framework for photon monte carlo treatment planning', *Phys. Med. Biol.* **52**, N425.

Franciosini, G., Battistoni, G., Cerqua, A., Gregorio, A. D., Maria, P. D., Simoni, M. D., Dong, Y., Fischetti, M., Marafini, M., Mirabelli, R., Muscato, A., Patera, V., Salvati, F., Sarti, A., Sciubba, A., Toppi, M., Traini, G., Trigilio, A. & Schiavi, A. (2023), 'Gpu-accelerated monte carlo simulation of electron and photon interactions for radiotherapy applications', *Phys. Med. Biol.* **68**(4), 044001.

Gaffney, D. K., Leavitt, D. D., Tsodikov, A., Smith, L., Watson, G., Patton, G., Gibbs, F. A. & Stewart, J. R. (2001), 'Electron arc irradiation of the postmastectomy chest wall with ct treatment planning: 20-year experience', *Int. J. Radiat. Oncol. Biol. Phys.* **51**, 994–1001.

Gauer, T., Sokoll, J., Cremers, F., Harmansa, R., Luzzara, M. & Schmidt, R. (2008), 'Characterization of an add-on multileaf collimator for electron beam therapy', *Phys. Med. Biol.* **53**, 1071.

Guyer, G., Mueller, S., Koechli, C., Frei, D., Volken, W., Bertholet, J., Mackeprang, P. H., Loebner, H. A., Aebersold, D. M., Manser, P. & Fix, M. K. (2022), 'Enabling non-isocentric dynamic trajectory radiotherapy by integration of dynamic table translations', *Phys. Med. Biol.* **67**.

Heath, E., Mueller, S., Guyer, G., Duetschler, A., Elicin, O., Aebersold, D., Fix, M. K. & Manser, P. (2021), 'Implementation and experimental validation of a robust hybrid direct aperture optimization approach for mixed-beam radiotherapy', *Med. Phys.* **48**, 7299–7312.

Heng, V. J., Serban, M., Seuntjens, J. & Renaud, M. A. (2021), 'Ion chamber and film-based quality assurance of mixed electron-photon radiation therapy', *Med. Phys.* **48**, 5382–5395.

Henzen, D., Manser, P., Frei, D., Volken, W., Neuenschwander, H., Born, E. J., Joosten, A., Loessl, K., Aebersold, D. M., Chatelain, C., Stampanoni, M. F. M. & Fix, M. K. (2014b), 'Beamlet based direct aperture optimization for mert using a photon mlc', *Med. Phys.* **41**, 121711.

Henzen, D., Manser, P., Frei, D., Volken, W., Neuenschwander, H., Born, E. J., Vetterli, D., Chatelain, C., Stampanoni, M. F. M. & Fix, M. K. (2014a), 'Monte carlo based beam model using a photon mlc for modulated electron radiotherapy', *Med. Phys.* **41**, 021714.

Hogstrom, K. R. & Almond, P. R. (2006), 'Review of electron beam therapy physics', *Phys. Med. Biol.* **51**, R455.

Jin, L., Eldib, A., Li, J., Emam, I., Fan, J., Wang, L. & Ma, C.-M. (2014), 'Measurement and monte carlo simulation for energy-and intensity-modulated electron radiotherapy delivered by a computer-controlled electron multileaf collimator', *J. Appl. Clin. Med. Phys* **15**.

Jin, L., Ma, C. M., Fan, J., Eldib, A., Price, R. A., Chen, L., Wang, L., Chi, Z., Xu, Q., Sherif, M. & Li, J. S. (2008), 'Dosimetric verification of modulated electron radiotherapy delivered using a photon multileaf collimator for intact breasts', *Phys. Med. Biol.* **53**, 6009.

Kawrakow, I. & Fippel, M. (2000), 'Vmc++, a fast mc algorithm for radiation treatment planning', *Use Comput. Radiat. Ther. 8th Int. Conf. (Heidelberg, Ger. ed W Schlegel T Bortfeld (heidelb. Springer)* pp. 126–128.

Khan, F. M., Fullerton, G. D., Lee, J. M., Moore, V. C. & Levitt, S. H. (1977), 'Physical aspects of electron-beam arc therapy', *Radiology* **124**, 497–500.

Klein, E. E., Vicic, M., Ma, C. M., Low, D. A. & Drzymala, R. E. (2008), 'Validation of calculations for electrons modulated with conventional photon multileaf collimators', *Phys. Med. Biol.* **53**, 1183.

Korevaar, E. W., Huizenga, H., Löf, J., Stroom, J. C., Leer, J. W. H. & Brahme, A. (2002), 'Investigation of the added value of high-energy electrons in intensity-modulated radiotherapy: four clinical cases', *Int. J. Radiat. Oncol. Biol. Phys.* **52**, 236–253.

Leavitt, D. D., Peacock, L. M., Gibbs, F. A. & Stewart, J. R. (1985), 'Electron arc therapy: Physical measurement and treatment planning techniques', *Int. J. Radiat. Oncol. Biol. Phys.* **11**, 987–999.

Leavitt, D. D. & Stewart, J. R. (1993), 'Electron arc therapy of the postmasectomy prosthetic breast', *Int. J. Radiat. Oncol. Biol. Phys.* **28**, 297–301.

Lewis, D. & Chan, M. F. (2015), 'Correcting lateral response artifacts from flatbed scanners for radiochromic film dosimetry', *Med. Phys.* **42**, 416–429.

Lewis, D., Micke, A., Yu, X. & Chan, M. F. (2012), 'An efficient protocol for radiochromic film dosimetry combining calibration and measurement in a single scan', *Med. Phys.* **39**, 6339–6350.

Li, J. G., Williams, S. S., Goffinet, D. R., Boyer, A. L. & Xing, L. (2000), 'Breast-conserving radiation therapy using combined electron and intensity-modulated radiotherapy technique', *Radiother. Oncol.* **56**, 65–71.

Ma, C. M., Pawlicki, T., Lee, M. C., Jiang, S. B., Li, J. S., Deng, J., Yi, B., Mok, E. & Boyer, A. L. (2000), 'Energy- and intensity-modulated electron beams for radiotherapy', *Phys. Med. Biol.* **45**, 2293–2311.

Ma, C., Parsons, D., Chen, M., Jiang, S., Hou, Q., Gu, X. & Lu, W. (2019), 'Electron modulated arc therapy (emat) using photon mlc for postmastectomy chest wall treatment i: Monte carlo-based dosimetric characterizations', *Phys. Med.* **67**, 1–8.

Manser, P., Frauchiger, D., Frei, D., Volken, W., Terribilini, D. & Fix, M. K. (2019), 'Dose calculation of dynamic trajectory radiotherapy using monte carlo', *Z. Med. Phys.* **29**, 31–38.

McNeely, L. K., Jacobson, G. M., Leavitt, D. D. & Stewart, J. R. (1988), 'Electron arc therapy: Chest wall irradiation of breast cancer patients', *Int. J. Radiat. Oncol. Biol. Phys.* **14**, 1287–1294.

Micke, A., Lewis, D. F. & Yu, X. (2011), 'Multichannel film dosimetry with nonuniformity correction', *Med. Phys.* **38**, 2523–2534.

Mihaljevic, J., Soukup, M., Dohm, O. & Alber, M. (2011), 'Monte carlo simulation of small electron fields collimated by the integrated photon mlc', *Phys. Med. Biol.* **56**, 829.

Mu, X., Olofsson, L., Karlsson, M., Sjögren, R. & Zackrisson, B. (2004), 'Can photon imrt be improved by combination with mixed electron and photon techniques?', *Acta Oncol.* **43**, 727–735.

Mueller, S., Fix, M. K., Henzen, D., Frei, D., Frauchiger, D., Loessl, K., Stampanoni, M. F. M. & Manser, P. (2018a), 'Electron beam collimation with a photon mlc for standard electron treatments', *Phys. Med. Biol.* **63**, 025017.

Mueller, S., Fix, M. K., Joosten, A., Henzen, D., Frei, D., Volken, W., Kueng, R., Aebersold, D. M., Stampanoni, M. F. & Manser, P. (2017), 'Simultaneous optimization of photons and electrons for mixed beam radiotherapy', *Phys. Med. Biol.* **62**, 5840–5860.

Mueller, S., Guyer, G., Risse, T., Tessarini, S., Aebersold, D. M., Stampanoni, M. F., Fix, M. K. & Manser, P. (2022), 'A hybrid column generation and simulated annealing algorithm for direct aperture optimization', *Phys. Med. Biol.* **67**, 075003.

Mueller, S., Guyer, G., Volken, W., Frei, D., Torelli, N., Aebersold, D. M., Manser, P. & Fix, M. K. (2023), 'Efficiency enhancements of a monte carlo beamlet based treatment planning process: implementation and parameter study', *Phys. Med. Biol.* **68**(4), 044003.

Mueller, S., Manser, P., Volken, W., Frei, D., Kueng, R., Herrmann, E., Elicin, O., Aebersold, D. M., Stampanoni, M. F. & Fix, M. K. (2018b), 'Part 2: Dynamic mixed beam radiotherapy (dymber): Photon dynamic trajectories combined with modulated electron beams', *Med. Phys.* **45**, 4213–4226.

Míguez, C., Jiménez-Ortega, E., Palma, B. A., Miras, H., Ureba, A., Arráns, R., Carrasco-Peña, F., Illescas-Vacas, A. & Leal, A. (2017), 'Clinical implementation of combined modulated electron and photon beams with conventional mlc for accelerated partial breast irradiation', *Radiother. Oncol.* **124**, 124–129.

Neph, R., Lyu, Q., Huang, Y., Yang, Y. M. & Sheng, K. (2021), 'Deepmc: a deep learning method for efficient monte carlo beamlet dose calculation by predictive denoising in magnetic resonance-guided radiotherapy', *Phys. Med. Biol.* **66**(3), 035022.

Neuenschwander, H., Mackie, T. R. & Reckwerdt, P. J. (1995), 'Mmc-a high-performance monte carlo code for electron beam treatment planning', *Phys. Med. Biol.* **40**, 543–574.

O'Shea, T. P., Ge, Y., Foley, M. J. & Faddegon, B. A. (2011), 'Characterization of an extendable multi-leaf collimator for clinical electron beams', *Phys. Med. Biol.* **56**(23), 7621.

Otto, K. (2008), 'Volumetric modulated arc therapy: Imrt in a single gantry arc', *Med. Phys.* **35**, 310–317.

Paddick, I. (2000), 'A simple scoring ratio to index the conformity of radiosurgical treatment plans', *J. Neurosurg.* **93 (Suppl 3)**, 219–222.

Palma, B. A., Sánchez, A. U., Salguero, F. J., Arráns, R., Sánchez, C. M., Zurita, A. W., Hermida, M. I. R. & Leal, A. (2012), 'Combined modulated electron and photon beams planned by a monte-carlo-based optimization procedure for accelerated partial breast irradiation', *Phys. Med. Biol.* **57**, 1191.

Renaud, M.-A., Serban, M. & Seuntjens, J. (2017), 'On mixed electron-photon radiation therapy optimization using the column generation approach', *Med. Phys.* **44**, 4287–4298.

Renaud, M.-A., Serban, M. & Seuntjens, J. (2019), 'Robust mixed electron-photon radiation therapy optimization', *Med. Phys.* **46**, 1384–1396.

Rodrigues, A., Yin, F. F. & Wu, Q. (2014), 'Dynamic electron arc radiotherapy (dear): A feasibility study', *Phys. Med. Biol.* **59**, 327–345.

Rosca, F. (2012), 'A hybrid electron and photon imrt planning technique that lowers normal tissue integral patient dose using standard hardware', *Med. Phys.* **39**, 2964–2971.

Salguero, F. J., Arrns, R., Palma, B. A. & Leal, A. (2010), 'Intensity- and energy-modulated electron radiotherapy by means of an xmlc for head and neck shallow tumors', *Phys. Med. Biol.* **55**, 1413.

Sharma, P. K., Jamema, S. V., Kaushik, K., Budrukkar, A., Jalali, R., Deshpande, D. D., Tambe, C. M., Sarin, R. & Munshi, A. (2011), 'Electron arc therapy for bilateral chest wall irradiation: Treatment planning and dosimetric study', *Clin. Oncol.* **23**, 216–222.

Surucu, M., Klein, E. E., Mamalui-Hunter, M., Mansur, D. B. & Low, D. A. (2010), 'Planning tools for modulated electron radiotherapy', *Med. Phys.* **37**, 2215–2224.

Teoh, M., Clark, C. H., Wood, K., Whitaker, S. & Nisbet, A. (2011), 'Volumetric modulated arc therapy: a review of current literature and clinical use in practice', *Br. J. Radiol.* **84**, 967–996.

Thomas, S. J. (2006), 'Margins between clinical target volume and planning target volume for electron beam therapy', *Brit. J. Radiol.* **79**(939), 244–247.

Unkelbach, J., Fabiano, S., Bennan, A. B. A., Mueller, S. & Bangert, M. (2022), 'Joint optimization of radiotherapy treatments involving multiple radiation modalities', *IEEE Trans. Radiat. Plasma Med. Sci.* **6**, 294–303.

Vatanen, T., Traneus, E. & Lahtinen, T. (2009), 'Comparison of conventional inserts and an add-on electron mlc for chest wall irradiation of left-sided breast cancer', *Acta Oncol.* **48**, 446–451.

Xiong, W., Li, J., Chen, L., Price, R. A., Freedman, G., Ding, M., Qin, L., Yang, J. & Ma, C. M. (2004), 'Optimization of combined electron and photon beams for breast cancer', *Phys. Med. Biol.* **49**, 1973.